Reactive Calcination Derived PZT Ceramics

A.M. AMER,* S.A. IBRAHIM, R.M. RAMADAN & M.S. AHMED

Department of Met. & Materials Eng. Faculty of Pet. & Min. Eng., Suez, Egypt

Abstract. Perovskite PZT ceramics are synthesized from stoichiometric oxide ratios of Pb, Zr, and Ti. The oxide powders are mixed mechanically and calcinated, and then sintered to form the desired perovskite phase using conventional solid-state reaction and reactive calcination routes. Highly reactive powders are produced by reacting the materials near the temperature of maximum volumetric expansion. At this point, an almost single phase with relatively high homogeneous structure is obtained. Also, the highly reactive powders allow densification to occur at temperatures as low as 950°C without the need to the additions of excess lead oxides. The dielectric properties of the PZT ceramics prepared by reactive calcination route are measured and compared with the conventional route.

Keywords: perovskite structure, PZT ceramics, dielectric constant, sintering

1. Introduction

Lead zirconate-titanate (PZT), a solid solution of ferroelectric PbTiO$_3$ ($T_c = 490°C$) and antiferroelectric PbZrO$_3$ ($T_c = 230°C$), belongs to the ferroelectric family of perovskite structure of a general formula ABO$_3$ (A = mono or divalent; B = tri or hexavalents ions) [1, 2]. PZT ceramics with compositions near to the morphotropic phase boundary (MPB) reveal excellent electromechanical properties due to the coexistence of the rhombohedral and tetragonal phases at room temperature. Cooling a PZT solid solution with a composition near the MPB below its Curie-temperature (T_c) induces a phase transformation from the paraelectric cubic (Pm3m) to the ferroelectric rhombohedral F_R (P3m) and ferroelectric tetragonal F_T (P4mm) modifications [3]. Investigations of the Pb(Zr$_x$ Ti$_{1-x}$)O$_3$ system have shown the existence of an almost temperature independent MPB at $x = 0.52$–0.53. X-rays diffraction indicated the co-existence of the two phases over a range of compositions around the MPB [4]. Many factors have been found to influence the non-uniformity of composition of PZT near the MPB, such as the raw powder particles size, surface area and purity. More

important however are process variables such as calcination and sintering temperatures and the method employed to minimize PbO loss. The volatility of the PbO component of PZT at high temperatures makes the stoichiometry difficult to control. Either an excess or a deficiency of PbO can degrade the intrinsic electromechanical properties. Excess PbO is usually added to compensate for loss of PbO during calcination and sintering, by reducing the concentrations of lead and oxygen vacancies. Therefore, it is desirable to process PZT and PZT-based ceramic materials at as low a temperature as possible, to alleviate, if not completely eliminate, these problems. One approach is the use of ultrafine ceramic powders as the starting materials, which may be synthesized via several chemistry-based novel preparation routes, such as the oxalate route [5], coprecipitation [6], hydrothermal reaction [7], and alkoxide hydrolysis (sol-gel) [8], to name a few of the many methodologies. However, most chemical synthesis techniques are relatively costly and do not lend themselves for mass production. Enhanced reactivity and subsequent densification of conventionally prepared Pb-based perovskites have been reported as being related to the calcination conditions [9]. Venkataramani [10] found that enhanced densification of PZT could be achieved by only partially reaction the component powders. The enhanced densification was believed to

*To whom all correspondence should be addressed. E-mail: Adelamer74@hotmail.com
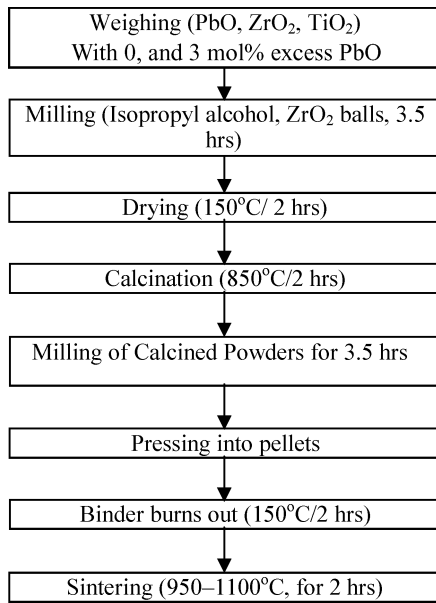
Weighing (PbO, ZrO$_2$, TiO$_2$)
With 0, and 3 mol% excess PbO

↓

Milling (Isopropyl alcohol, ZrO$_2$ balls, 3.5 hrs)

↓

Drying (150°C/ 2 hrs)

↓

Calcination (850°C/2 hrs)

↓

Milling of Calcined Powders for 3.5 hrs

↓

Pressing into pellets

↓

Binder burns out (150°C/2 hrs)

↓

Sintering (950–1100°C, for 2 hrs)

Fig. 1. Conventional one-stage solid-state reaction process flow chart for the PZT ceramics.

be the result of a reactive sintering process which occurred during the final stages of perovskite formation. Although no explanation was given, Takagi et al. [11] observed enhanced densification for partially calcined Pb-rich surface layer on the B-site component oxides.
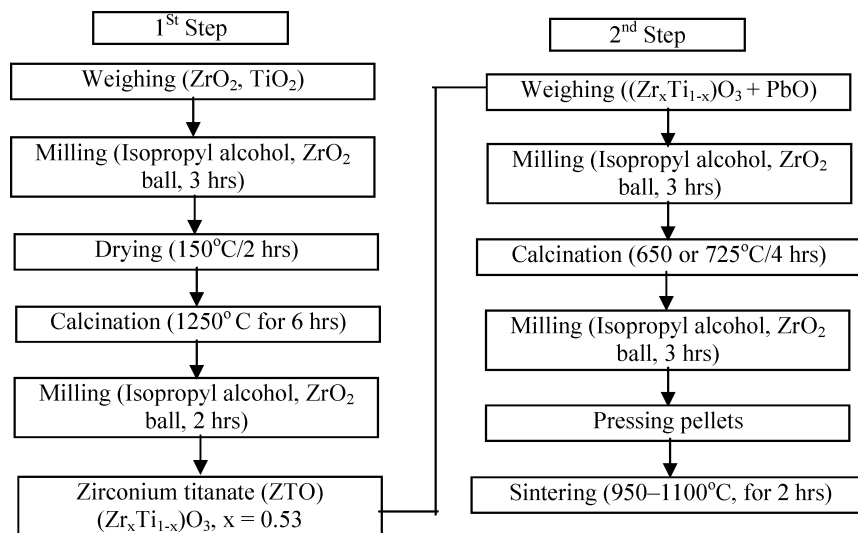
The objective of this work is to evaluate the reactive calcination technique as a simple alternative procedure and compared it to the conventional solid state reaction route. The influence of calcination and sintering temperatures on the crystalline structure of the two co-existent phases in a PZT solid solution with $x = 0.53$. Proposed mechanism for enhanced densification is also discussed.

2. Experimental Procedure

2.1. Samples Preparation

Stoichiometric and 3-mol% PbO excess PZT samples (Pb(Zr$_{0.53}$Ti$_{0.47}$)O$_3$) with a fixed Zr/Ti ratio of 53/47 were prepared by the conventional mixed-oxide and reactive calcination routes. The general processing steps of the MPB PZT production by the two different routes are shown in Figs. 1 and 2. The starting raw materials were commercially available powders in oxide form of high purity: PbO (99%, Riedel Dehaen CO.), TiO$_2$ (99.4%, Degussa Co.), ZrO$_2$ (99.7%, Strem Chemical Co.). The calcined powders were consolidated into green compacts of 7.5 mm diameter and 2–3 mm thickness by using a hard steel die and cold uniaxially pressing of 690 MPa with water as a binder. Sintering was performed in air atmosphere with a mixture of (PbZrO$_3$ + 10 mol% ZrO$_2$) powder bed in order to establish a constant PbO Vapor pressure during densification [12].

1St Step		2nd Step
Weighing (ZrO$_2$, TiO$_2$)		Weighing ((Zr$_x$Ti$_{1-x}$)O$_3$ + PbO)
↓		↓
Milling (Isopropyl alcohol, ZrO$_2$ ball, 3 hrs)		Milling (Isopropyl alcohol, ZrO$_2$ ball, 3 hrs)
↓		↓
Drying (150°C/2 hrs)		Calcination (650 or 725°C/4 hrs)
↓		↓
Calcination (1250°C for 6 hrs)		Milling (Isopropyl alcohol, ZrO$_2$ ball, 3 hrs)
↓		↓
Milling (Isopropyl alcohol, ZrO$_2$ ball, 2 hrs)		Pressing pellets
↓		↓
Zirconium titanate (ZTO) (Zr$_x$Ti$_{1-x}$)O$_3$, x = 0.53	→	Sintering (950–1100°C, for 2 hrs)

Fig. 2. Improved two-stage solid-state (reactive calcination) reaction process flow chart of the PZT ceramics.

2.2. Powder Characterization

The calcined and sintered samples were examined by XRD using a Siemens D500 X-ray diffractometer. The voltage and currents rating used were 40 Kv, 30 mA respectively, and Cu K_α radiation was used. The relative density measurements were determined by the Archimedes method. Electrical properties measurements were carried by sputter depositing silver paste as an electrode on both sides of the specimens. The capacitance, C (Farad) and, the dissipation factor (tanδ) were measured at different frequencies of 100 Hz and 1 kHz at room temperature in order to estimated the dielectric constant (ε_r) [13] of the various produced materials.

3. Results and Discussion

3.1. Conventional Solid-State Route

Sintered powders were examined by X-ray diffractmeter to ensure phase purity and to identify the phases and lattice constants of the materials. Figure 3 presents

XRD patterns for stoichiometric composition of calcined PZT Ceramics at 850°C/2 h and sintered at temperatures ranging from 950° to 1100°C. The sintered samples at 950°C, exhibited a similar XRD spectrum to calcined powder at 850°C, with appearance of other extra small peaks most likely belonging to the precipitation of ZrO_2 as shown in Fig. 3(a). The presence of ZrO_2 at this stage can be related to the evaporation of lead oxide during sintering, which moved the composition to the Ti-rich PZT region. Also, it is important to note that the rhombohedral-tetragonal (RT) phase transition started at this temperature [14]. The observed triple splitting peaks are considered as an evidence for the tetragonal and rhombohedral phase co-existence. A gradual change to a double peaks splitting is observed with increasing sintering temperatures, Fig. 3(b) and (c). This could well indicate that, a transformation of the mixture of tetragonal and rhombohedral phases to an almost single tetragonal phase increases with sintering temperature. Also it is noted that, all peaks are shifted to higher angle values with increasing sintering temperatures. A similar phenomenon was reported in the previous studies [14, 15]. It suggests that this phenomenon is transition related. The lattice
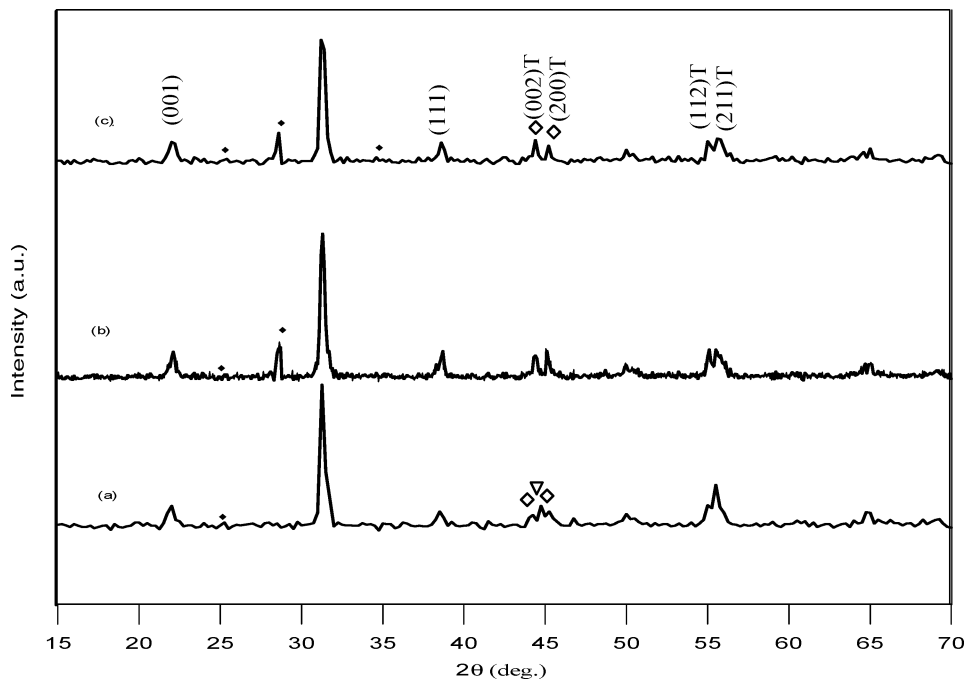

Fig. 3. XRD patterns for stoichiometric composition of calcined PZT ceramics at 850°C/2 h and sintered at: (a) 950°C/2 h, (b) 1000°C/2 h, (c) 1100°C/2 h (♦: ZrO_2, ◇: Tetragonal phase, ▽: Rhombohedral phase).
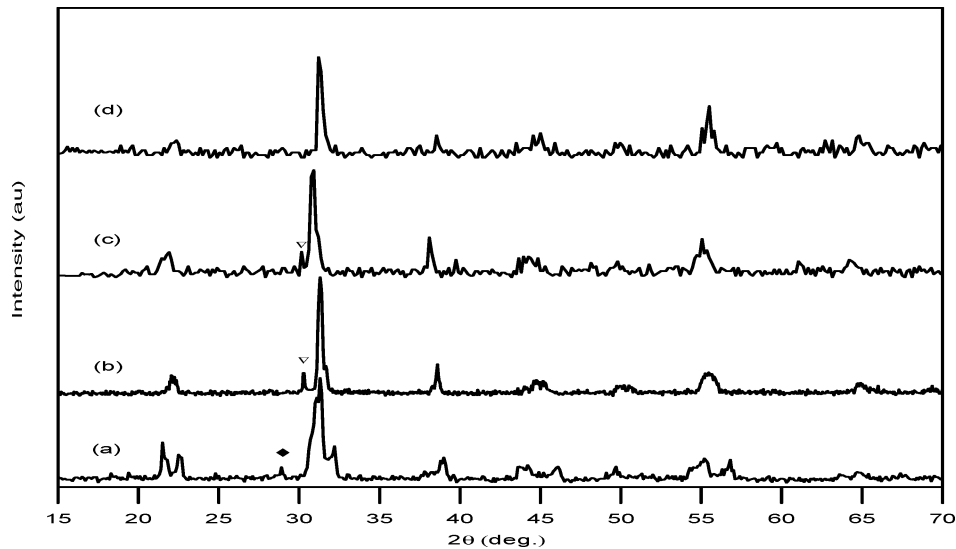
Fig. 4. XRD patterns for 3 mol% excess lead oxide composition of PZT ceramics: (a) calcined at 850°C/2 h and sintered at (b) 950°C/2 h, (c) 1000°C/2 h, (d) 1100°C/2 h (♦: PbTiO$_3$, ▽: PbO).

parameters of the two coexisting ferroelectric phases in the samples were calculated from the triplets (200). The results obtained for (Pb(Zr$_{0.53}$Ti$_{0.47}$)O$_3$) solids solutions showed that the lattice parameters of the tetragonal phase changed with sintering temperature. The value of the a_T parameter decreased from 0.4052 to 0.3974 nm and the c_T value slightly decreased from 0.4144 to 0.4070 nm when the sintering temperature increased from 950° to 1100°C. The axial ratio c_T/a_T increased from 1.0227 to 1.0240 in the investigated temperature range, showing that distortion of the tetragonal unit cell from the basic perovskite cell is higher at higher sintering temperatures. It is also an indication to the increasing of the amount of tetragonal phase as compared to rhombohedral phase.

On other hand, the diffraction pattern of calcined powder with 3 mol% excess PbO at 850°C is shown in Fig. 4(a). A similar XRD spectrum to calcined stoichiometric PZT composition at the same temperature is obtained, and a few lines of PT (PbTiO$_3$) are observed e.g. at $2\theta = 28.8°$, which is believed to originate from the uncompleted reaction during powder calcination.

The sintered samples at 950°C, exhibit almost a similar XRD spectrum to the calcined powder in spite of the disappearance of lead titanate (PbTiO$_3$) peaks as shown in Fig. 4(b). It is also observed that the tetragonal to rhombohedral transition started at this temperature and a small extra peak of PbO phase is observed

at $2\theta = 30.2°$. By increasing the sintering temperature at 1000 and 1100°C, the positions of the two tetragonal peaks, e.g. (002) and (200), tend to move closer to the rhombohedral peak, which slightly oscillates about a mean position. This means that the rhombohedral phase in the specimen with 3 mol% excess PbO is likely to be dominating, as shown in Fig. 4(c) and (d). It also observed that the tetragonal lattice parameter a_T increased from 0.401 to 0.4030 nm and the c_T value slightly decreased from 0.4104 to 0.4064 nm with increasing sintering temperature. The axial ratio c_T/a_T decreases almost linearly from 1.023 to 1.009, in an investigated temperatures range, showing that the distortion of the basic perovskite cell is lower as the sintering temperature increases. The rhombohedral lattice parameter a_R is almost constant, with increasing sintering temperature.

On other hand, the resulting values for the lattice parameter a_T is in a fairly good agreement with those previously found in Pb(Zr$_x$Ti$_{1-x}$)O$_3$ system with $x = 0.53$ and prepared by various technological conditions [16, 17]. Conversely c_T values are slightly lower than those previously reported for unmodified PZT solid solution [16]. The distortion of the rhombohedral cell from an ideal perovskite one is lower than that of the tetragonal cell, the parameter a_R oscillating in a very narrow range from 0.4080 to 0.4082 nm. In previous work [18] a_R is also found to change in the range

from 0.407 to 0.4084 nm. The value of 0.408 nm can be assigned to the cubic cell of the paraelectric phase [19]. This means that the presence of excess PbO compensate for lead loss during sintering and structure is vary closed to the stoichiometric composition.

3.2. Reactive Calcination Route

It is generally suggested that a highly reactive powder could be achieved by partially reacting the component materials near the temperature of maximum volumetric expansion [9, 11]. This corresponding expansion is believed to be associated with the formation of phases possessing a larger molar volume than the individual components of the reaction, which leads to rapid coarsening of the highly reactive product layer resulting in a porous-type structure. Based on this concept, many attempts are carried out to produce the perovskite $Pb(Zr_x Ti_{1-x})O_3$ structure. In this process, it is possible to avoid the formation of intermediate reaction when starting from individual oxides. This can be achieved by pretreated of B-site (Zr, or Ti) cations using the method developed by Shrout [20]. Following calcination treatment for ZrO_2 and TiO_2 mixture, the product is mixed with PbO powder before further calcination at either 650° or 725°C, Fig. 2.

The stoichiometric composition diffraction pattern after 4 h calcination at 650°C is shown in Fig. 5(a)

and compared with excess lead sample composition, Fig. 5(b). It is possible to observe that the number of PbO peaks is less compared with sample containing 3 mol% excess PbO calcined under the same conditions, Fig. 5(b). This result could well indicate that the perovskite phase formation is not complete for both compositions.

Increasing calcination temperature to 725°C, the reaction is observed to be almost complete and the perovskite structure (tetragonal) is dominating in XRD pattern, Fig. 6(a), for the stoichiometric composition. On the other hand, the composition of excess PbO-PZT ceramics showed a few PbO-peaks in diffraction pattern in addition to the tetragonal lines, Fig. 6(b). It appears that excess lead has a retard effect on the reaction rate.

The results of the sintering processes that are carried at two temperatures of 950 and 1100°C for both compositions after different calcination temperatures are shown in Figs. 7 and 8 indicates a structure-dependence on both calcination temperatures as well as the composition. For the sintered stoichiometric composition at 950°C, a mixed perovskite structures of T and R phases are observed as shown in Fig. 7(a). While with increasing sintering temperature to 1100°C resulted in an almost single tetragonal phase, as shown in Fig. 7(b). The composition with excess lead content is shown in Fig. 8(a) dominate with a mixed structure of tetragonal and rhombohedral phases after sintering at 950°C. A
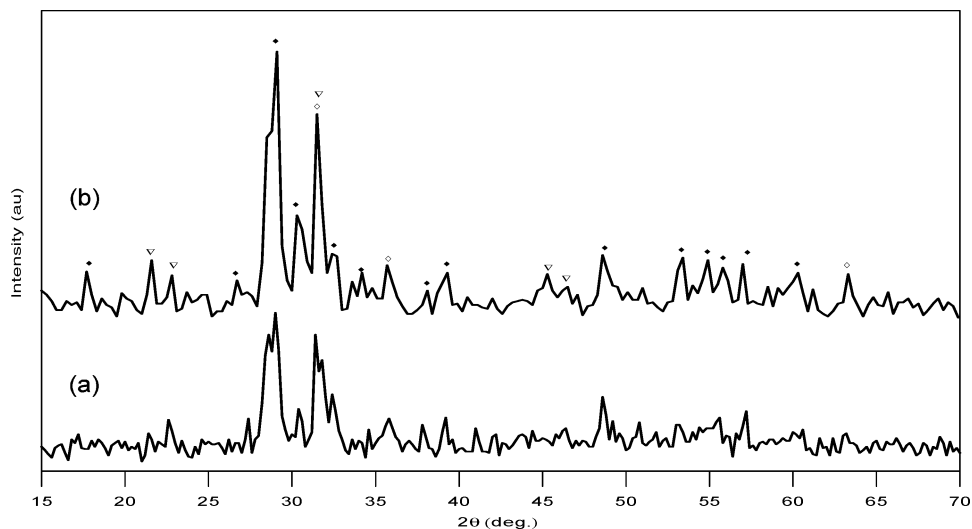

Fig. 5. XRD patterns of PZT ceramics calcined at 650°C/4 h for: (a) Stoichiometric composition and, (b) 3 mol% excess PbO (♦: PbO, ◊: (Zr, Ti)O_2, ▽: PZT).
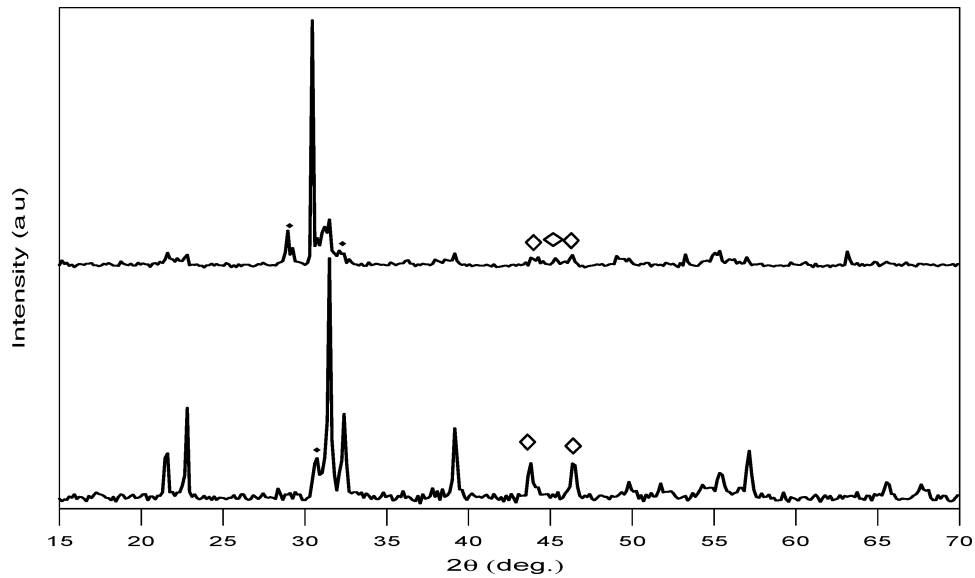
Fig. 6. XRD patterns of PZT ceramics calcined at 725°C/4 h for: (a) Stoichiometric composition and, (b) 3 mol% exces PbO (♦: PbO, ◇: *T*. phase, ◇: *R*. phase).
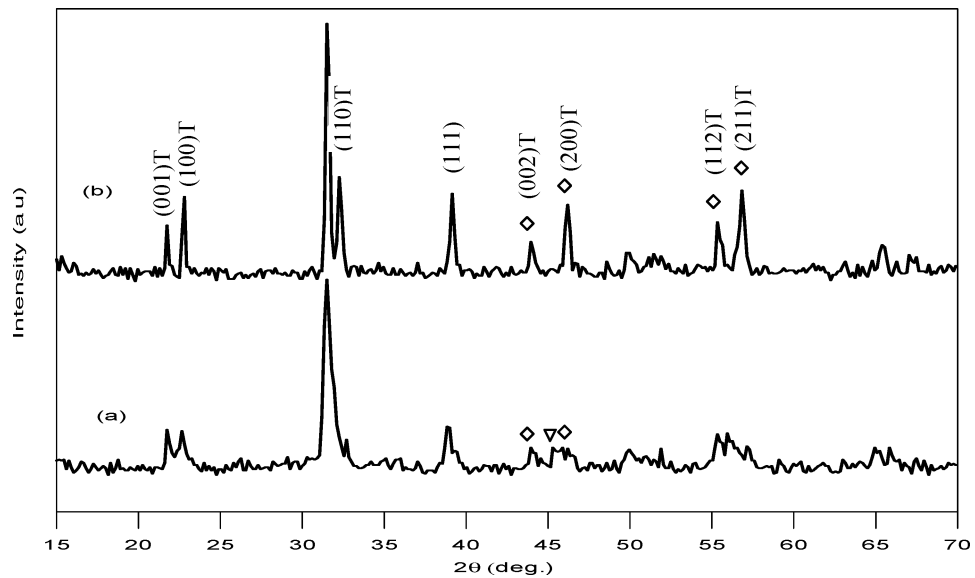

Fig. 7. XRD patterns of the stoichiometric composition of PZT ceramics calcined at 650°C/4 h and sintered at: (a) 950°C/2 h, (b) 1100°C/2 h (◇: *T* phase, ∇: *R* phase).

transformation to almost complete rhombohedral structure is observed at the higher sintering temperature of 1100°C, as shown in Fig. 8(b). The presence of a mixed structure *T* and *R* phases is a strong indication of the material inhomogeneity and excess lead in the second composition is responsible for the composition shift

that leads to structure transformation from tetragonal to rhombohedral at high sintering temperature.

Structural changes are also observed during sintering at various temperatures of the pre-calcined samples at 725°C. The stoichiometric composition shows, Fig. 9(a) and (b) a dominating tetragonal perovskite
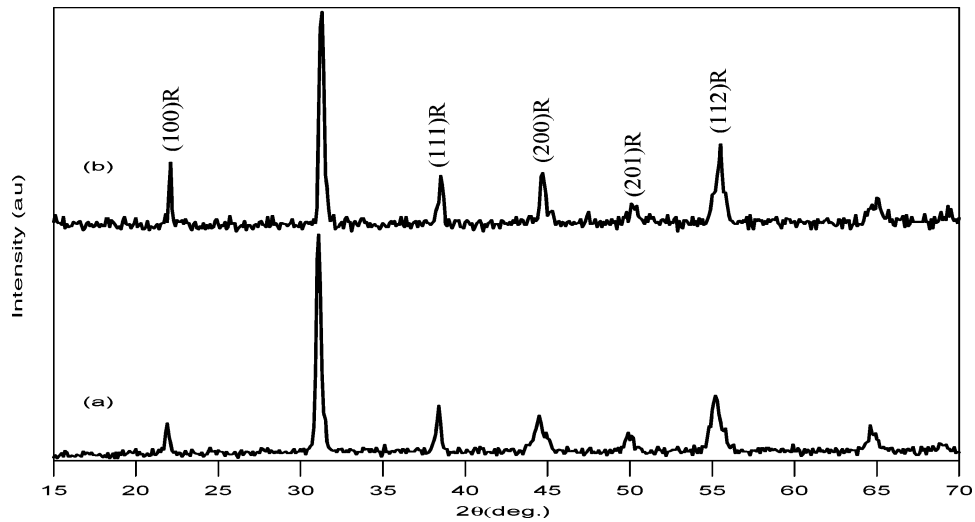
Fig. 8. XRD patterns for 3 mol% excess lead oxide composition of the calcined PZT ceramics at 650°C/4 h and sintered at: (a) 950°C/2 h, (b) 1100°C/2 h.
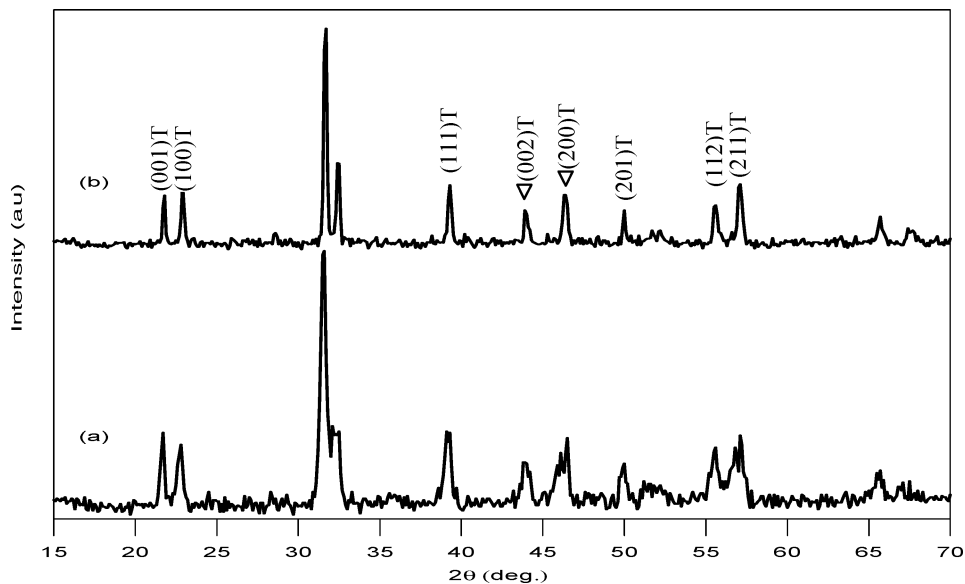

Fig. 9. XRD patterns of the stoichiometric composition PZT ceramics calcined at 725°C/4 h and sintered at: (a) 950°C/2 h, (b) 1100°C/2 h (∇: *T* phase).

structure after sintering at both temperature of 950 and 1100°C. However, the excess lead samples yielded a rather rhombohedral at higher sintering temperatures as shown in Fig. 10(b), and a mixed structures of *T* and *R* phases at lower one, as shown in Fig. 10(a). It is clear that the composition difference have an important role in determining the final produced structure mainly during calcination as well as the type of the structure dominating at the final sintering temperature. It is obvious that calcination temperature of 650°C does not correspond to the maximum volumetric expansion of the produced materials; even when excess lead is added to the stoichiometric composition. However, improvements in the reactivity rate
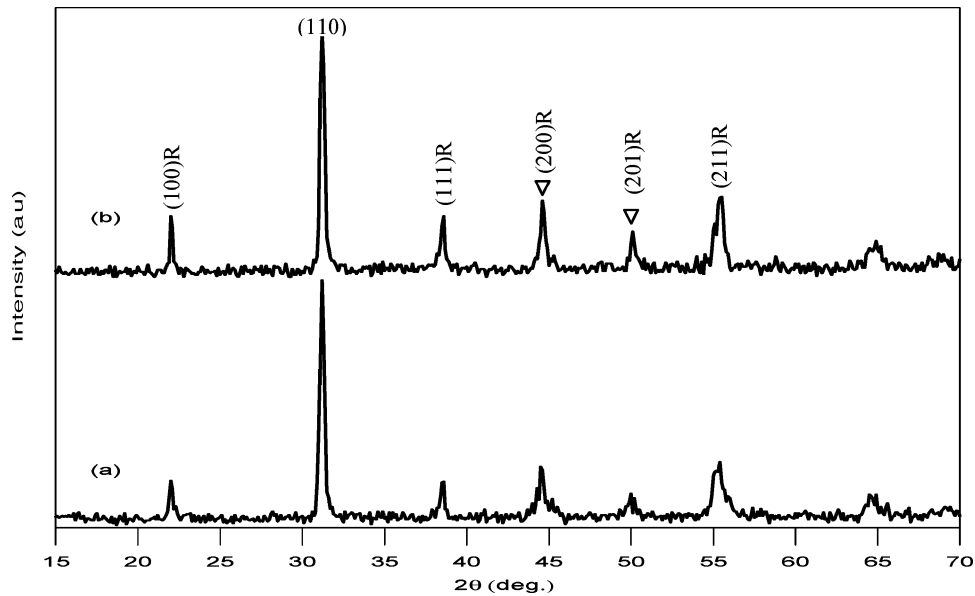
Fig. 10. XRD patterns for 3 mol% excess lead oxide composition of the calcined PZT ceramics at 725°C/4 h and sintered at: (a) 950°C/2 h, (b) 1100°C/2 h (∇: *R* phase).

can be obtained by raising the calcination temperature to 725°C.

3.3. Densification During Sintering

Densification of all samples is characterized by the relative densities. Table 1 represents the relative densities of the stoichiometric and 3-mol% PbO excess PZT samples that were prepared by the conventional mixed-oxide and reactive calcination routes. The results indicated that the density of stoichiometric composition of PZT ceramic prepared by the conventional mixed-

oxide route has a relative small increase in their values with sintering temperatures with maximum at 1100°C. Excess PbO-content samples showed a slightly higher value of the relative density especially at 950°C which may be due the presence of liquid phase as excess PbO is presented. Furthermore, at lower sintering temperature a relatively higher density values are obtained in general for compositions with excess lead compared to the stoichiometric one. On other hand, since there no significant difference in the relative densities after sintering could be observed, Table 1, between the two compositions that were prepared by reactive calcination route, the role of excess lead addition for

Table 1. The physical and electrical properties of the PZT ceramics.

Conditions and Properties	Conventional mixed oxides route				Reactive calcination route			
Composition	St. Comp.		Excess PZT		St. Comp.		Excess PZT	
Cal. temp. (°C)	850	850	850	850	725	725	725	725
Sin. temp. (°C)	950	1100	950	1100	950	1100	950	1100
R. density (%)	94	95.8	95.7	95	94.5	95.5	95.3	95.1
Dielectric constant								
100 Hz	995	927	972	1127	1055	1123	969	1002
1 kHz	950	884	905	1060	1026	1046	929	954
Dissipation factor								
100 Hz	0.027	0.030	0.028	0.025	0.021	0.018	0.035	0.033
1 kHz	0.038	0.44	0.040	0.0303	0.026	0.027	0.045	0.041

compensating Pb-loss is no more needed in this reactive method. The improved two-stage solid reaction process has also an important advantage by regard to the conventional one-stage solid-state reaction process that the final sintering temperature could be reduced by about 100–200°C. Since a single phase structure could be obtained at 950–1100°C, while a higher temperature is need for the conventional powder method.

Table 1 also shows the dielectric properties as represented by dielectric constant (relative permittivity ε_r) and, the dissipation factor (tanδ) as a function of sintering temperature. It observed that, with increasing frequency dielectric constant values decrease, whereas dielectric loss slowly increases. Moreover, the dielectric constant values of the stoichiometric PZT ceramics prepared by conventional solid-state route decrease with increasing sintering temperature. This may be due to the presence of second phase (ZrO_2), which is considered as antiferroelectric phase, and increases with increasing sintering temperatures. while, the values of dielectric constant of excess PbO-PZT materials increases with increasing sintering temperature and the maximum values of dielectric constant is observed for the composition with 3 mol% excess PbO after sintering at 1100°C. On other hand, a maximum dielectric constant values are obtained for stoichiometric PZT ceramics prepared by reactive calcination route.

4. Conclusion

(1) Conventional solid-state route through both calcination and sintering processes have used to produce PZT ceramics and the optimum conditions of this powder route are determine in order to have a highly compacted material with minimum porosity. A 3-mol% PbO excess is also found to be a suitable amount addition to have the perovskite structure without second phase precipitation.

(2) The mixture of two phases, tetragonal and rhombohedral perovskite structure, are determine and their evolution are also followed through various stages of preparation. The degree of tetragonality distortion, c_T/a_T ratio, is found to Zr/Ti ratio dependent.

(3) An almost single phase perovskite structure of PZT ceramics of fine particles has been successfully prepared via reactive calcination route from the low-cost, widely available oxides without the need to excess lead oxide additions.

(4) The use of reactive calcination route allows the preparation of dense and relatively homogeneous PZT at lower sintering temperature of 950°C that is convenient for lead volatilization limitation.

(5) Dielectric constant of the prepared PZT ceramics and their density are comparable with the expected from their nominal composition.

References

1. J. Mal and R.P. Choudhary, *J. Phys. Chem. Solids*, **58**(3), 421 (1997).
2. T.L. Jordan and Z. Ounaies, *ICASE, NASA Langley Research Center* (Hampton, Virginia, 2001), p. 2.
3. B. Jaffe, R. Roth, and S. Marzullo, *J. Appl. Phys.*, **25**(6), 809 (1954).
4. K. Kakegawa, O. Matsunaga, T. Kato, and Y. Sasaki, *J. Am. Ceram. Soc.*, **78**(4), 1071 (1995).
5. E. Leite, M. Cerqueira, L. Perazoli, R. Nasar, and J. Varela, *J. Am. Ceram. Soc.*, **79**(6), 1563 (1995).
6. Hong-Wen Wang, David A. Hall, and Frank R. Sale, *J. Am. Ceram. Soc.*, **75**(1), 124 (1992).
7. H. Cheng, J. Ma, B. Zhu, and Y. Cui, *J. Am. Ceram. Soc.*, **76**(3), 625 (1993).
8. A. Amer, S. Ibrahim, M. Ahmed, and M. Ramadan, in *8th Inter. Conference on Mining, Petroleum and Metallurgical Eng. Suez Canal University*, Egypt, 2003, pp. 43–53.
9. T. Shrout, P. Papet, S. Kim, and G. Lee, *J. Am. Ceram. Soc.*, **73**(7), 1862 (1990).
10. S. Venkataramani, Ph.D. Thesis, The Pennsylvania State University, University Park, 1981.
11. T. Takagi, K. Anetami, and K. Shimiza, U.S. Pat. No. 4, 1989, p. 426.
12. B. Hiremath, A. Kingon, and J. Biggers, *J. Am. Ceram. Soc.*, **66**(11), 790 (1983).
13. R.C. Buchanan, *Ceramic Materials for Electronic, Processing, Properties and Applications* (Marcel Dekker, Inc., New York, 1986).
14. Zhang, H. Uusimaki, S. Leppavuori, and Karijalainen, *J. Appl. Phys.* **76**(7), 4294 (1994).
15. L. Hanh, K. Uchino, and S. Namura, *J. Jpn. Appl. Phys.*, **17**(4), 637 (1978).
16. K. Kakegawa, K. Arai, Y. Sasaki, and T. Tomizawa, *J. Am. Ceram. Soc.*, **77**(1), C49 (1988).
17. S.A. Mabud, *J. Appl. Crystallogr.*, **13**(3), 211 (1980).
18. P. Gr, Lucuta, *J. Am. Ceram. Soc.*, **68**(10), 533 (1985).
19. F. Vasiliu, P. Luctra, and F. Constantinescu, *Phys. Stat. Sol.*, **80**, 637 (1983).
20. S. Swartz and T. Shrout, *Mater. Res. Bull.*, **17**, 1245 (1982).